


Current Fluctuations in Nanopores Reveal the Polymer-Wall Adsorption Potential

Stuart F. Knowles¹,¹ Nicole E. Weckman¹,¹ Vincent J. Y. Lim¹,¹ Douwe J. Bonthuis²,²
Ulrich F. Keyser¹,¹ and Alice L. Thorneywork^{1*}

¹*Cavendish Laboratory, Department of Physics, University of Cambridge,
JJ Thomson Avenue, Cambridge CB3 0HE, United Kingdom*

²*Institute of Theoretical and Computational Physics,
Graz University of Technology, 8010 Graz, Austria*

 (Received 15 February 2021; accepted 19 August 2021; published 23 September 2021)

Modification of surface properties by polymer adsorption is a widely used technique to tune interactions in molecular experiments such as nanopore sensing. Here, we investigate how the ionic current noise through solid-state nanopores reflects the adsorption of short, neutral polymers to the pore surface. The power spectral density of the noise shows a characteristic change upon adsorption of polymer, the magnitude of which is strongly dependent on both polymer length and salt concentration. In particular, for short polymers at low salt concentrations no change is observed, despite the verification of comparable adsorption in these systems using quartz crystal microbalance measurements. We propose that the characteristic noise is generated by the movement of polymers on and off the surface and perform simulations to assess the feasibility of this model. Excellent agreement with experimental data is obtained using physically motivated simulation parameters, providing deep insight into the shape of the adsorption potential and underlying processes. This paves the way toward using noise spectral analysis for *in situ* characterization of functionalized nanopores.

DOI: [10.1103/PhysRevLett.127.137801](https://doi.org/10.1103/PhysRevLett.127.137801)

Resistive pulse sensing with nanoscale pores is a powerful technique for studying single molecules [1–3], with applications as varied as sub-Angstrom particle sizing [4], DNA sequencing [5], and digital data storage [6]. For many years, however, nanopores have also offered fundamental insights into polymer transport in confined environments [7]. For example, ionic current trace measurements have been used to quantify polymer partitioning into biological pores, such as α -hemolysin and alamethicin, providing information on the pore structure and size [8–10]. Significant additional information can also be obtained from the fluctuations, or noise, in the ionic current trace, which reflects dynamic properties of molecules in the pore, such as diffusion coefficients [11,12].

Whether employed for fundamental or applied purposes, understanding nanopore surface properties is essential, since they can dominate behavior due to the small length scales of such systems [13]. When sensing with solid-state pores, practical problems associated with the pore surface include nonspecific interactions between the analyte and pore, and physical effects such as electro-osmotic flow (EOF), which can inhibit analyte transport [14–16]. Here, polymers have found applications as surface coatings to reduce these undesirable features and even introduce new functionality, e.g., to mimic gating [17]. Coatings can be formed chemically, by covalently bonding polymers to the pore wall or created physically, by passive adsorption of polymers to the surface [18]. Benefits of the latter include

simpler formation and possible coating regeneration [19]. Using passive adsorption to generate robust surface coatings with desired features is not trivial, however, as the attachment of the polymer to the surface is much less controlled than with grafting. For example, polymer loop length is highly sensitive to adsorption kinetics and difficult to predict analytically [20–24]. Yet models suggest that EOF suppression by adsorbed polymers requires a polymer conformation with loops extending away from the surface [25,26], making this a crucial parameter in experimental design.

Furthermore, the effects of passively adsorbed polymer layers on the noise properties of the pore have only been studied in certain cases [27]. Noise in nanopore systems is known to be dominated by surface properties [28,29], and these may be modified by adsorption. Understanding any such change is key for sensing techniques, because increased noise can reduce resolution and sensitivity. Moreover, noise changes may provide valuable information into the physical adsorption process itself [30].

Here, we explore the effect of adsorbed polymer layers on the noise properties of glass nanopores. We quantify the noise by calculation of the power spectral density (PSD) for the same glass nanopore before and after addition of polyethylene glycol (PEG) to the electrolyte solution. By considering the behavior in KCl solutions of varying concentrations and with PEG molecules of different lengths, we find that following the addition of PEG,

fluctuations below 10 kHz are greatly increased in systems with higher salt concentrations and longer PEG molecules. However, at the lowest salt concentration considered (50 mM) and with shorter PEG molecules, no change in fluctuations was observed. Quartz crystal microbalance with dissipation monitoring (QCM D) experiments were performed to confirm that PEG adsorbs in all cases. We simulate fluctuations in the numbers of adsorbed polymers and obtain excellent agreement with experiment, leading us to conclude that the excess noise sensitively reflects the adsorption-desorption process. Additionally, quantitative matching between simulation and experiment allows us to infer the range and depth of the polymer-wall adsorption potential.

Glass nanopores [31] with a nominal diameter of 16 ± 2 nm were mounted into poly-dimethylsiloxane (PDMS) chips, as described previously [29]. For each measurement the chip is first filled with KCl solution at pH 6, and a current trace is measured at 500 mV. Next, the reservoir holding the capillary tips is flushed with the same salt solution now containing PEG (Merck) [32] at a concentration of 0.04% w/w, sufficiently diluted such that polymer-polymer interactions can be neglected, and any change in solution conductivity is undetectable. A large negative voltage (-500 mV) is applied across the pore for 5 minutes, to induce EOF directed into the pore [33] and thus pull PEG molecules inside [Fig 1(a)]. Current traces are then rerecorded, to allow direct quantification of the effects of PEG on the noise properties of the pore while controlling for pore-to-pore variations. Further details of the experimental protocols can be found in the Supplemental Material [34], which contains Refs. [35–41].

Figure 1(b) shows short sections of current traces from nanopores in 50 mM and 500 mM KCl, both before and after the addition of PEG 8000. In 50 mM KCl, the current traces appear to be very similar, whereas in 500 mM KCl, the noise markedly increases upon addition of PEG. The corresponding PSDs of the current fluctuations for the four traces in Fig. 1(b) are shown in Fig. 1(c), and further demonstrate that, while for 50 mM KCl the current fluctuations do not change upon addition of PEG, at 500 mM KCl a striking difference is observed. In particular, the magnitude of the PSD is significantly increased between ~ 0.5 Hz and 5 kHz, with over an order of magnitude difference occurring at ~ 10 Hz. For higher frequencies ($\gtrsim 30$ kHz, full curves shown in the Supplemental Material [34]), the two PSD curves coincide again, consistent with previous work showing that high-frequency noise is dominated by capacitive effects [3,29]. From here, we refer to the spectra before the addition of PEG as S_0 .

A natural question is whether the observation of no change in the PSD implies no PEG adsorption. To address this, the adsorption of PEG molecules to quartz glass was also studied using QCM D measurements. Here, solutions

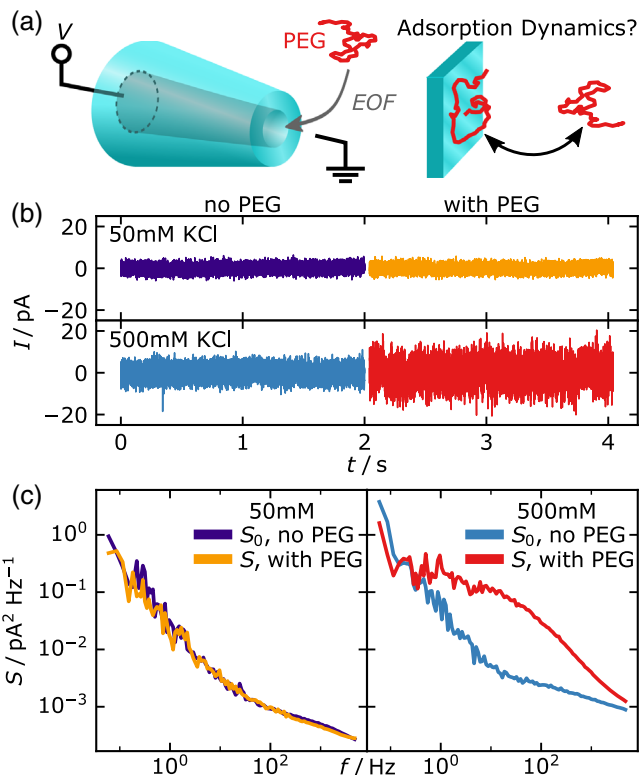


FIG. 1. Measuring changes in ionic current noise upon introducing PEG into a glass nanopore. (a) Experimental schematic illustrating the insertion of polymer molecules (PEG) into the pore using EOF. (b) Short sections of the ionic current traces before and after the introduction of PEG into solution. The traces are digitally filtered to a 5 kHz bandwidth and centered to their own mean current to emphasize differences in noise properties. (c) Concomitant changes in the power spectral density of the noise.

containing PEG are flowed across a quartz crystal, and changes in the crystal's resonant frequency and dissipation, which reflect adsorption to the crystal, are monitored. Crucially, the quartz crystals used in QCM D are the same material as the nanopores, the surfaces are prepared in the same manner for both experiments, and the same concentrations of PEG are used, allowing us to infer from the QCM D results the likely adsorption process in the nanopore. Fig. 2 shows both the frequency (ΔF) and dissipation (ΔD) shift curves for solutions of PEG 8000 in 50 mM and 500 mM KCl, corresponding to the spectra in Fig. 1. At $t = 10$ minutes, a drop in the ΔF curve and an increase in the ΔD curve correspond to the arrival of the solution containing PEG and adsorption of PEG to the surface. Notably, there is excellent agreement between the curves at the two different salt concentrations with respect to both ΔD and ΔF . This implies not only that similar amounts of PEG adsorb (agreement in the ΔF curves), but also that the adsorbed PEG has similar conformations in both situations (agreement in the ΔD curves, see the Supplemental Material [34]). The QCM D measurements thus confirm

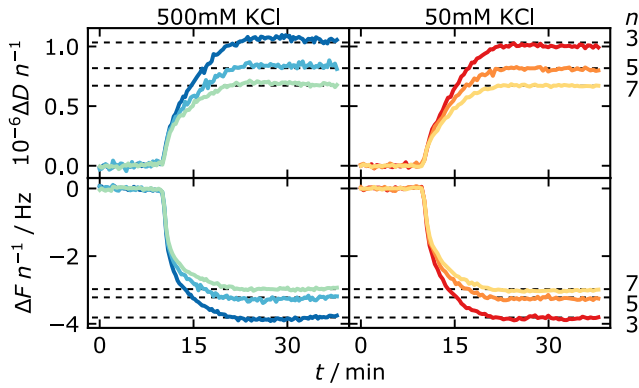


FIG. 2. Verifying PEG adsorption with QCM D. Frequency (ΔF) and dissipation (ΔD) shifts from QCM D measurements for $50 \mu\text{M}$ PEG 8000 in 50 mM (right) and 500 mM (left) KCl solutions. Three harmonics are shown, all rescaled by their harmonic number n .

that the variation in noise is not due to differing adsorption in different salt concentrations; however, they do not provide any information on the dynamics of the adsorption process or the origins of the noise.

Having established that a lack of excess noise does not reflect an absence of adsorbed PEG, we next explore the excess noise variation with the length of the PEG molecules. In the top panel of Fig. 3, we plot the PSD for systems at an intermediate KCl concentration of 150 mM, but with PEG molecules of varying length at a constant monomer concentration (weight percent). The top panel of Fig. 3 clearly shows that increasing the length of PEG increases the excess noise. Moreover, at this intermediate salt concentration the excess noise for PEG 8000 is present, though less than in 500 mM salt [Fig 1(c)], highlighting the

sensitivity of the excess noise to relatively small changes in conditions.

To uncover excess noise variation more clearly, in the bottom panel of Fig. 3, we plot the difference $S - S_0$ for all combinations of salt concentration and PEG length. The spectra have been curtailed to the frequency domain in which they are well defined, i.e., where $S \gg S_0$, and curves for PEG 1000 and PEG 8000 in 50 mM KCl are not shown, since in those cases no change in noise is observed. The shape of the excess noise is characteristic and well approximated by a curve of the form

$$S_{\text{model}}(f) = \frac{A}{1 + (f/f_0)^\gamma} \quad (1)$$

with A the amplitude of the spectrum, f_0 the corner frequency, and γ the limiting slope at high frequencies. From fits of Eq. (1) to the excess noise spectra in the bottom panel of Fig. 3, we find that $\gamma < 1.4$, but does not vary strongly across the spectra considered. In contrast, f_0 decreases with increasing PEG length, as shown by the range of f_0 values marked in gray for each panel.

The range of corner frequencies, $f_0 \sim 10\text{--}100$ Hz, in Fig. 3 implies a characteristic timescale for the noise-generating process on the order of milliseconds. This immediately rules out both polymer conformation variation and ionic association-dissociation as the origin of this noise, since these processes have nanosecond timescales [42]. While Eq. (1) also describes the PSD for the fluctuations in the number of particles diffusing in a channel [11], these would be an order of magnitude faster than the fluctuations we observed and, moreover, are predicted to have $\gamma \gtrsim 1.5$. In contrast, a mechanism involving polymer adsorption-desorption from the walls could be consistent with our

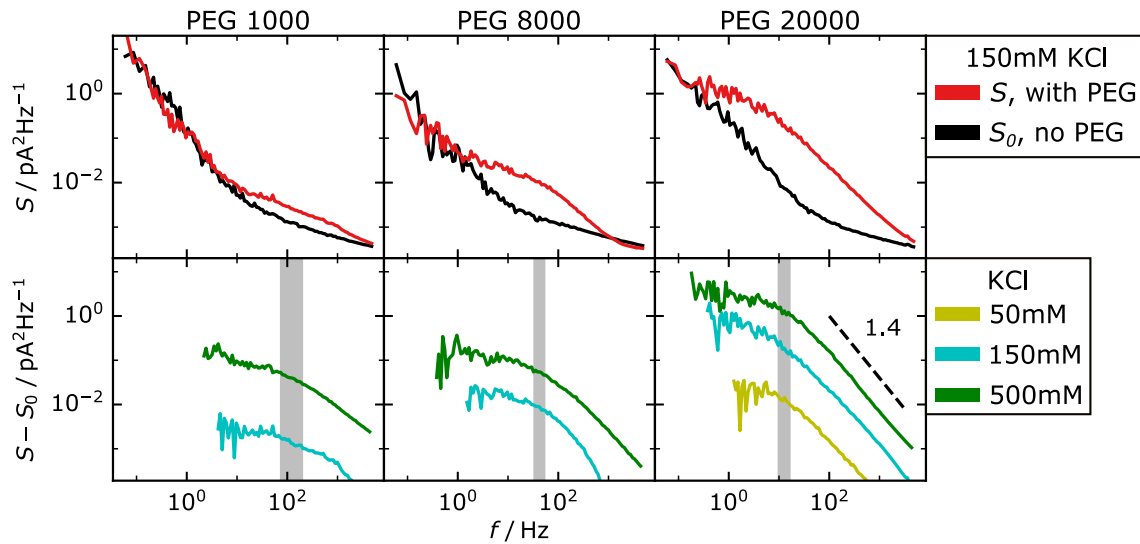


FIG. 3. Top: The effect of PEG length on excess noise. Spectra are shown for PEGs 1000, 8000, and 20 000 in 150 mM KCl. Bottom: The excess noise, $S - S_0$, for all systems. Curves are shown only for frequencies where $S_0 < S$. The range of corner frequencies obtained by fitting to Eq. (1) are shown in gray. A typical limiting slope of 1.4 is marked.

experimental observations, including the characteristic timescales. For weak and reversible surface adsorption, a polymer will locally block surface current. Even with many polymers adsorbed, the net change in current is likely to be negligible. The movement of polymers on and off the surface could increase current fluctuations measurably, however, leading to the observed change in the PSD. This is consistent with the coincidence of S and S_0 at low frequencies, which implies that the change in noise is due to a mechanism not present in the bare pore, rather than an enhancement of an existing effect. Additionally, this is also reliant on the polymers being isolated on the surface to allow desorption in contrast to dense layers, e.g., those formed from polymer melts [24].

This proposed mechanism, however, assumes particular details of the adsorption dynamics that are not known *a priori* and cannot be inferred from the QCMD results. To assess the feasibility of this hypothesis, we use Monte Carlo simulations to study fluctuations in the number of adsorbed particles for a cylindrical channel with reversible adsorption to the surface via a square well adsorption potential:

$$V_{\text{sim}} = \begin{cases} -\alpha & r < r^* \\ 0 & \text{otherwise} \end{cases} \quad (2)$$

with α the adsorption energy for the whole chain in units of $k_B T$ and r^* the adsorption range. Note that the channel wall is at $r = 0$ and the center at $r = R$, as shown in the inset in Fig. 4. This is the simplest viable model for our system:

polymer chains are coarse grained such that only the time evolution of the polymer's center of mass position is considered, without any polymer-polymer interactions. Additionally the adsorption potential form is dependent on only two input parameters, and the slight taper of the nanopore ($\sim 4^\circ$) is neglected. Full simulation details are given in the Supplemental Material [34], containing Refs. [43–45]. Fluctuations in the particle number are simulated for various values of α and r^* , and from these traces we obtain PSDs with the same functional form as that observed in the experimental excess noise spectra in Fig. 3. Fitting the spectra to Eq. (1) allows the dependence of the corner frequency f_0 and high-frequency exponent γ on the simulation parameters—adsorption range and energy—to be explored.

Figure 4(a) shows the variation of f_0 and γ with r^* and α . Both f_0 and γ decrease with increasing adsorption range and energy. These dependencies are, however, much weaker for γ , with all values of $\alpha \sim 3-4k_B T$ consistent with the experimental data. In contrast, the strong dependence of the corner frequency on r^* puts clear constraints on the adsorption range. In particular, for PEG 20 000 r^* must be approximately 6 nm, close to the radius of gyration for PEG 20 000, $R_g \approx 6.2$ nm [39]. If we take this constraint on r^* , we require $\alpha \approx 3k_B T$. Extending this logic to the other PEG weights, we see that the experimental requirements on f_0 for PEGs 1000 and 8000 with $\alpha = 3k_B T$ can be satisfied by $r^* = 1.2$ nm and 3.8 nm—the respective radii of gyration. Importantly, these values of α and r^* , consistent with the experimental data, support our proposed mechanism of weak and reversible adsorption.

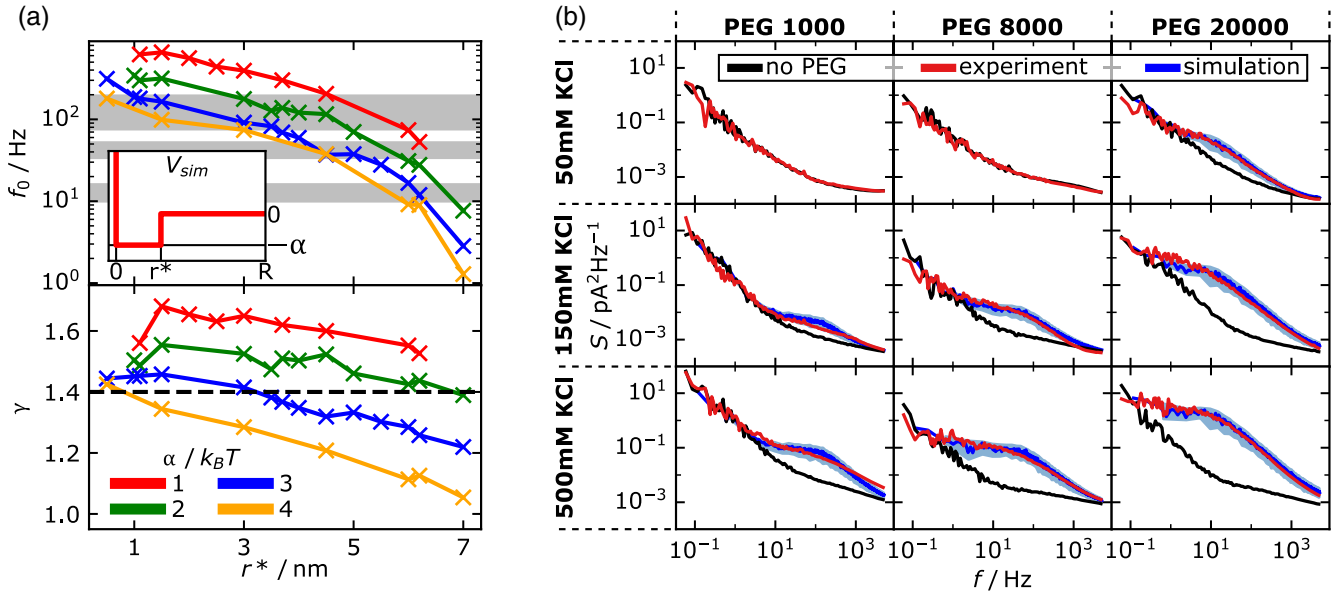


FIG. 4. (a) Variation of the corner frequency f_0 and limiting exponent γ , with adsorption potential parameters α and r^* (inset), obtained from simulated spectra. Experimental ranges of f_0 for each PEG weight are shown in gray (top), and the observed limit of $\gamma \sim 1.4$ is marked (bottom). (b) Comparison of experimental (red and black) and simulated (blue) spectra, for all parameter combinations. Confidence intervals for simulated spectra are shaded. Columns have constant PEG weight and rows have constant salt concentration, as indicated.

In Fig. 4(b), we show the experimental spectra with a global fit obtained from the simulations for all combinations of PEG weight and salt concentration considered. Here the simulation curves are obtained by combining the simulated PSD for the fluctuations in the number of adsorbed polymers using $r^* = R_g$ and $\alpha = 3k_B T$ with the experimental spectra for the system with no PEG. Excellent agreement is obtained between the experiment and simulations in all cases, further validating the model.

Finally, when fitting the simulations to our experiment, we leave the fitting parameter, A in Eq. (1) as a free parameter. The value of A accounts for the scaling between number and current fluctuations, and depends on the average current change on adsorption of a single polymer. This in turn depends on not only the surface charge density, but also the ensemble and relative probabilities of all the conformational microstates of the polymer on the surface. This would be prohibitively difficult to predict from first principles, so we do not attempt to draw quantitative conclusions from the values we obtain for A , instead focusing on the trends. The increase of A with salt concentration can be understood from the increased current density at higher salt; current fluctuations can be associated with the adsorbed polymer blocking an area of current density within the pore, with the current change thus proportional to the current density in the blocked area. Over the salt concentrations considered here, the current density (both surface and bulk) scales approximately linearly with salt concentration (see the Supplemental Material), so we would expect $A \propto c^2$. That A increases with polymer length can be understood from geometric effects, i.e., larger polymers blocking a greater area. These trends suggest that the absence of excess noise for PEGs 1000 and 8000 in 50 mM KCl does not indicate that the polymer-generated noise is absent, but that in those conditions it is negligible when compared with the intrinsic noise of the pore, which is independent of c [29].

In conclusion, we have investigated the effect of adsorbed polymers on the noise properties of glass nanopores by systematic study of the PSD of ionic current fluctuations. For PEG 8000 in 500 mM KCl, a characteristic increase in the spectral density was found on addition of PEG; however, when the salt concentration was lowered, the excess noise ceased to be observed. This prompted further investigation into the relationship between excess noise and experimental conditions. QCM D measurements confirmed that the PEG molecules adsorb in all cases, ruling out the possibility that the lack of noise increase is due to a lack of adsorbed polymer. Simulations confirmed our hypothesis that the noise arose from fluctuations in the number of adsorbed polymers, with such excellent agreement using this simple model of our system strongly suggesting that adsorption-desorption processes are at

the core of the excess noise. Notably, this approach allowed us to quantitatively determine the range and depth of the adsorption potential for a single polymer interacting with the surface ($r^* = R_g$ and $\alpha = 3-4k_B T$).

This Letter elucidates the relationship between adsorbed polymer layers in solid-state nanopores and the ionic current noise properties of those pores. This will facilitate better design of sensing experiments, for example, with polymer layers tailor made to reduce EOF whilst minimizing excess noise. Furthermore, we have shown that noise analysis is a powerful tool for assessing nanoscale dynamics, with unrealized potential in the creation of functionalized nanopores, both as physical models of biological pores and as advanced single-molecule sensors.

S. F. K. acknowledges funding from UK Research and Innovation – Engineering and Physical Sciences Research Council (UKRI, EPSRC) and the EPSRC CDT in Nanoscience and Nanotechnology (NanoDTC). N. W. acknowledges funding from Oxford Nanopore Technologies, the Canada-UK Foundation, and the University of Cambridge Office of Postdoctoral Affairs. D. J. B. acknowledges financial support from the Anschubfinanzierung funding scheme of the TU Graz (12th call). U. F. K. acknowledges support from an ERC consolidator grant (Designerpores No. 647144). A. L. T. acknowledges support from the University of Cambridge Ernest Oppenheimer Fund.

*at775@cam.ac.uk

- [1] C. Dekker, Solid-state nanopores, *Nat. Nanotechnol.* **2**, 209 (2007).
- [2] T. Albrecht, Single-molecule analysis with solid-state nanopores, *Annu. Rev. Anal. Chem.* **12**, 371 (2019).
- [3] A. Fragasso, S. Schmid, and C. Dekker, Comparing current noise in biological and solid-state nanopores, *ACS Nano* **14**, 1338 (2020).
- [4] M. A. Edwards, S. R. German, J. E. Dick, A. J. Bard, and H. S. White, High-speed multipass Coulter counter with ultrahigh resolution, *ACS Nano* **9**, 12274 (2015).
- [5] J. Quick, N. J. Loman, S. Duraffour, J. T. Simpson, E. Severi, L. Cowley, J. A. Bore, R. Koundouno, G. Dudas, A. Mikhail *et al.*, Real-time, portable genome sequencing for Ebola surveillance, *Nature (London)* **530**, 228 (2016).
- [6] K. Chen, J. Kong, J. Zhu, N. Ermann, P. Predki, and U. F. Keyser, Digital data storage using DNA nanostructures and solid-state nanopores, *Nano Lett.* **19**, 1210 (2019).
- [7] S. M. Bezrukov, I. Vodyanoy, and V. Adrian Parsegian, Counting polymers moving through a single ion channel, *Nature (London)* **370**, 279 (1994).
- [8] S. M. Bezrukov, I. Vodyanoy, R. A. Brutyan, and J. J. Kasianowicz, Dynamics and free energy of polymers partitioning into a nanoscale pore, *Macromolecules* **29**, 8517 (1996).

- [9] T. K. Rostovtseva, E. M. Nestorovich, and S. M. Bezrukov, Partitioning of differently sized poly (ethylene glycol)s into OmpF porin, *Biophys. J.* **82**, 160 (2002).
- [10] E. M. Nestorovich, V. A. Karginov, and S. M. Bezrukov, Polymer partitioning and ion selectivity suggest asymmetrical shape for the membrane pore formed by epsilon toxin, *Biophys. J.* **99**, 782 (2010).
- [11] S. M. Bezrukov, A. M. Berezhkovskii, M. A. Pustovoit, and A. Szabo, Particle number fluctuations in a membrane channel, *J. Chem. Phys.* **113**, 8206 (2000).
- [12] S. Marbach, D. S. Dean, and L. Bocquet, Transport and dispersion across wiggling nanopores, *Nat. Phys.* **14**, 1108 (2018).
- [13] D. P. Hoogerheide, S. Garaj, and J. A. Golovchenko, Probing Surface Charge Fluctuations with Solid-State Nanopores, *Phys. Rev. Lett.* **102**, 256804 (2009).
- [14] S. Van Dorp, U. F. Keyser, N. H. Dekker, C. Dekker, and S. G. Lemay, Origin of the electrophoretic force on DNA in solid-state nanopores, *Nat. Phys.* **5**, 347 (2009).
- [15] M. Firmkes, D. Pedone, J. Knezevic, M. Doblinger, and U. Rant, Electrically facilitated translocations of proteins through silicon nitride nanopores: Conjoint and competitive action of diffusion, electrophoresis, and electroosmosis, *Nano Lett.* **10**, 2162 (2010).
- [16] M. Boukhet, F. Piguet, H. Ouldali, M. Pastoriza-Gallego, J. Pelta, and A. Oukhaled, Probing driving forces in aerolysin and α -hemolysin biological nanopores: Electrophoresis versus electroosmosis, *Nanoscale* **8**, 18352 (2016).
- [17] R. Brilmayer, C. Förster, L. Zhao, and A. Andrieu-Brunsen, Recent trends in nanopore polymer functionalization, *Curr. Opin. Biotechnol.* **63**, 200 (2020).
- [18] E. A. S. Doherty, K. Derek Berglund, B. A. Buchholz, I. V. Kourkine, T. M. Przybycien, R. D. Tilton, and A. E. Barron, Critical factors for high-performance physically adsorbed (dynamic) polymeric wall coatings for capillary electrophoresis of DNA., *Electrophoresis* **23**, 2766 (2002).
- [19] E. A. S. Doherty, R. J. Meagher, M. N. Albarghouthi, and A. E. Barron, Microchannel wall coatings for protein separations by capillary and chip electrophoresis, *Electrophoresis* **24**, 34 (2003).
- [20] C. A. J. Hoeve, E. A. DiMarzio, and P. Peyser, Adsorption of polymer molecules at low surface coverage, *J. Chem. Phys.* **42**, 2558 (1965).
- [21] P.-G. De Gennes, *Scaling Concepts in Polymer Physics* (Cornell University Press, Ithaca, 1979).
- [22] M. A. Cohen Stuart, T. Cosgrove, and B. Vincent, Experimental aspects of polymer adsorption at solid/solution interfaces, *Adv. Colloid Interface Sci.* **24**, 143 (1985).
- [23] A. N. Semenov and J.-F. Joanny, Structure of adsorbed polymer layers: Loops and tails, *Europhys. Lett.* **29**, 279 (1995).
- [24] S. Napolitano, Irreversible adsorption of polymer melts and nanoconfinement effects, *Soft Matter* **16**, 5348 (2020).
- [25] O. A. Hickey, J. L. Harden, and G. W. Slater, Molecular Dynamics Simulations of Optimal Dynamic Uncharged Polymer Coatings for Quenching Electro-Osmotic Flow, *Phys. Rev. Lett.* **102**, 108304 (2009).
- [26] N. Ermann, N. Hanikel, V. Wang, K. Chen, N. E. Weckman, and U. F. Keyser, Promoting single-file DNA translocations through nanopores using electro-osmotic flow, *J. Chem. Phys.* **149**, 163311 (2018).
- [27] S. Awasthi, P. Sriboonpeng, C. Ying, J. Houghtaling, I. Shorubalko, S. Marion, S. J. Davis, L. Sola, M. Chiari, A. Radenovic *et al.*, Polymer coatings to minimize protein adsorption in solid-state nanopores, *Small Methods* **4**, 2000177 (2020).
- [28] A. Fragasso, S. Pud, and C. Dekker, 1/f noise in solid-state nanopores is governed by access and surface regions, *Nanotechnology* **30**, 395202 (2019).
- [29] S. F. Knowles, U. F. Keyser, and A. L. Thorneywork, Noise properties of rectifying and non-rectifying nanopores, *Nanotechnology* **31**, 10LT01 (2020).
- [30] E. Kaätelhön, K. J. Krause, P. S. Singh, S. G. Lemay, and B. Wolfrum, Noise characteristics of nanoscaled redox-cycling sensors: Investigations based on random walks, *J. Am. Chem. Soc.* **135**, 8874 (2013).
- [31] R. A. Levis and J. L. Rae, The use of quartz patch pipettes for low noise single channel recording, *Biophys. J.* **65**, 1666 (1993).
- [32] J. Milton Harris, *Poly (Ethylene Glycol) Chemistry: Biotechnical and Biomedical Applications* (Springer Science & Business Media, New York, 2013).
- [33] R. B. Schoch, J. Han, and P. Renaud, Transport phenomena in nanofluidics, *Rev. Mod. Phys.* **80**, 839 (2008).
- [34] See Supplemental Material at <http://link.aps.org/supplemental/10.1103/PhysRevLett.127.137801> for further details of the experimental and simulation protocols.
- [35] L. J. Steinbock, O. Otto, D. R. Skarstam, S. Jahn, C. Chimere, J. L. Gornall, and U. F. Keyser, Probing dna with micro-and nanocapillaries and optical tweezers, *J. Phys. Condens. Matter* **22**, 454113 (2010).
- [36] N. Bell, DNA origami nanopores and single molecule transport through nanocapillaries, Ph.D. thesis, University of Cambridge, 2013.
- [37] N. Laohakunakorn, Electrokinetic phenomena in nanopore transport, Ph.D. thesis, 2015.
- [38] V. Yu. Zitserman, K. S. Stojilkovich, S. M. Bezrukov, and A. M. Berezhkovskii, Electrical conductivity of aqueous solutions of polyethylene glycol, *Russ. J. Phys. Chem. A* **79**, 1083 (2005), <https://science.nichd.nih.gov/confluence/download/attachments/39157791/RussJPC.pdf>.
- [39] K. Devanand and J. C. Selser, Asymptotic behavior and long-range interactions in aqueous solutions of poly (ethylene oxide), *Macromolecules* **24**, 5943 (1991).
- [40] K. A. Rubinson and S. Krueger, Poly (ethylene glycol)s 2000–8000 in water may be planar: A small-angle neutron scattering (SANS) structure study, *Polymer* **50**, 4852 (2009).
- [41] P. A. Gurnev, C. B. Stanley, M. A. Aksoyoglu, K. Hong, V. A. Parsegian, and S. M. Bezrukov, Poly (ethylene glycol) s in semidilute regime: Radius of gyration in the bulk and partitioning into a nanopore, *Macromolecules* **50**, 2477 (2017).

- [42] S. Gravelle, R. R. Netz, and L. Bocquet, Adsorption kinetics in open nanopores as a source of low-frequency noise, *Nano Lett.* **19**, 7265 (2019).
- [43] K. Kikuchi, M. Yoshida, T. Maekawa, and H. Watanabe, Metropolis Monte Carlo method as a numerical technique to solve the Fokker-Planck equation, *Chem. Phys. Lett.* **185**, 335 (1991).
- [44] M. J. Skaug, J. N. Mabry, and D. K. Schwartz, Single-molecule tracking of polymer surface diffusion, *J. Am. Chem. Soc.* **136**, 1327 (2014).
- [45] C. Yu, J. Guan, K. Chen, S. C. Bae, and S. Granick, Single-molecule observation of long jumps in polymer adsorption, *ACS Nano* **7**, 9735 (2013).